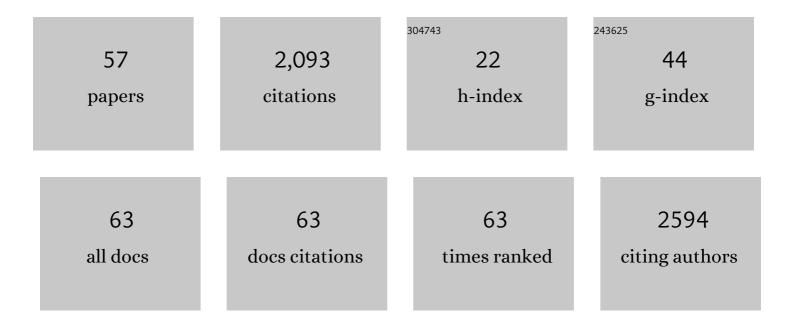
List of Publications by Year in descending order

Source: https://exaly.com/author-pdf/4911958/publications.pdf Version: 2024-02-01



MING GUO

#	Article	IF	CITATIONS
1	Effects of polystyrene microplastics on the seed germination of herbaceous ornamental plants. Science of the Total Environment, 2022, 809, 151100.	8.0	36
2	Eco-friendly soy protein isolate-based films strengthened by water-soluble glycerin epoxy resin. Progress in Organic Coatings, 2022, 162, 106566.	3.9	8
3	Effect of microwave/hydrothermal combined ionic liquid pretreatment on straw: Rumen anaerobic fermentation and enzyme hydrolysis. Environmental Research, 2022, 205, 112453.	7.5	17
4	Hyperbranched Molecularly Imprinted Photoactive Polymers and Its Detection of Tetracycline Antibiotics. ACS Applied Polymer Materials, 2022, 4, 1234-1242.	4.4	5
5	Synthesis, properties and applications of selfâ€repairing carbohydrates as smart materials via thermally reversible DA bonds. Polymers for Advanced Technologies, 2021, 32, 1026-1037.	3.2	3
6	Insights from nanotechnology in COVID-19 treatment. Nano Today, 2021, 36, 101019.	11.9	146
7	Delivery Mechanism of the Pharmaceutical Complex of Genisteinâ€Adenine Based on Spectroscopic and Molecular Modelling at Atomic Scale. Chemistry and Biodiversity, 2021, 18, e2000944.	2.1	1
8	Recent advance in the C–F bond functionalization of trifluoromethyl-containing compounds. Organic Chemistry Frontiers, 2021, 8, 3915-3942.	4.5	122
9	Electrocatalytic Properties of a Novel β-PbO ₂ /Halloysite Nanotube Composite Electrode. ACS Omega, 2021, 6, 5436-5444.	3.5	9
10	Targeting Hypoxic Tumors with Hybrid Nanobullets for Oxygen-Independent Synergistic Photothermal andÂThermodynamic Therapy. Nano-Micro Letters, 2021, 13, 99.	27.0	64
11	Noncovalent-bonded 3D Cd(II) and Zn(II) supramolecular metal-organic frameworks from 3,3′,5,5′-tetramethyl-4,4′-bipyrazole and carboxylates. Journal of Coordination Chemistry, 2021, 74, 1106-1123.	2.2	4
12	Molecularly imprinted polymer-based photocatalyst for highly selective degradation of methylene blue. Environmental Research, 2021, 194, 110684.	7.5	24
13	Preparation of biological sustained-release nanocapsules and explore on algae-killing properties. Journal of Advanced Research, 2021, 31, 87-96.	9.5	10
14	Production of magnetic sodium alginate polyelectrolyte nanospheres for lead ions removal from wastewater. Journal of Environmental Management, 2021, 289, 112506.	7.8	26
15	Electrochemical sensor based on corncob biochar layer supported chitosan-MIPs for determination of dibutyl phthalate (DBP). Journal of Electroanalytical Chemistry, 2021, 897, 115549.	3.8	23
16	Construction of supramolecular laccase enzymes and understanding of catalytic dye degradation using multispectral and molecular docking approaches. Reaction Chemistry and Engineering, 2021, 6, 1940-1949.	3.7	2
17	Chlorinated phosphorus flame retardants exert oxidative damage to SMMC-7721 human hepatocarcinoma cells. Science of the Total Environment, 2020, 705, 135777.	8.0	12
18	A Molecularly Imprinted Fluorescence Sensor Based on the ZnO Quantum Dot Core–Shell Structure for High Selectivity and Photolysis Function of Methylene Blue. ACS Omega, 2020, 5, 20664-20673.	3.5	10

#	Article	IF	CITATIONS
19	Biobased Epoxies Derived from Myrcene and Plant Oil: Design and Properties of Their Cured Products. ACS Omega, 2020, 5, 28918-28928.	3.5	4
20	Fighting Immune Cold and Reprogramming Immunosuppressive Tumor Microenvironment with Red Blood Cell Membrane-Camouflaged Nanobullets. ACS Nano, 2020, 14, 17442-17457.	14.6	190
21	Anti-tumor effect of synthetic baicalin-rare earth metal complex drugs on SMMC-7721 cells. Environmental Geochemistry and Health, 2020, 42, 3851-3864.	3.4	2
22	Effect of lignin degradation product sinapyl alcohol on laccase catalysis during lignin degradation. Industrial Crops and Products, 2019, 139, 111544.	5.2	22
23	Perfluorooctanoic acid exposure induces apoptosis in SMMC-7721 hepatocellular cancer cells. Environmental Pollution, 2019, 247, 509-514.	7.5	18
24	A facile route to synthesize hyperbranched polyester derived from cellulose and serine and its biodegradability. Reactive and Functional Polymers, 2019, 140, 62-71.	4.1	2
25	The polyaminocarboxylated modified hydrochar for efficient capturing methylene blue and Cu(II) from water. Bioresource Technology, 2019, 275, 360-367.	9.6	79
26	Atomic-scale investigation of the interaction between coniferyl alcohol and laccase for lignin degradation using molecular dynamics simulations and spectroscopy. Journal of Dispersion Science and Technology, 2019, 40, 686-694.	2.4	5
27	Removal of methylene blue from aqueous solution by modified bamboo hydrochar. Ecotoxicology and Environmental Safety, 2018, 157, 300-306.	6.0	154
28	A facile synthesis of molecularly imprinted polymers and their properties as electrochemical sensors for ethyl carbamate analysis. RSC Advances, 2018, 8, 39721-39730.	3.6	11
29	Synthesis of switchable intelligent molecularly imprinted polymers with selective adsorption of ethyl carbamate and their application in electrochemical sensor analysis. RSC Advances, 2018, 8, 25636-25644.	3.6	6
30	Effects of triazole fungicides on androgenic disruption and CYP3A4 enzyme activity. Environmental Pollution, 2017, 222, 504-512.	7.5	118
31	Nine supramolecular assemblies from 5,7-dimethyl-1,8-naphthyridine-2-amine and carboxylic acids by strong classical H-bonds and other noncovalent associations. Journal of Molecular Structure, 2017, 1150, 595-613.	3.6	5
32	Comparison of the interaction between lactoferrin and isomeric drugs. Spectrochimica Acta - Part A: Molecular and Biomolecular Spectroscopy, 2017, 173, 593-607.	3.9	16
33	Recent Advances on Endocrine Disrupting Effects of UV Filters. International Journal of Environmental Research and Public Health, 2016, 13, 782.	2.6	114
34	α-Mangostin Extraction from the Native Mangosteen (Garcinia mangostana L.) and the Binding Mechanisms of α-Mangostin to HSA or TRF. PLoS ONE, 2016, 11, e0161566.	2.5	28
35	Crystal Structures of Three Organic Adducts Produced by N6-Benzyladenine, Trichloroacetic Acid, 3-Nitrophthalic Acid, and Citric Acid. Journal of Chemical Crystallography, 2016, 46, 399-410.	1.1	5
36	Promoting Artemisinin Biosynthesis in Artemisia annua Plants by Substrate Channeling. Molecular Plant, 2016, 9, 946-948.	8.3	24

#	Article	IF	CITATIONS
37	Characterization of the Interaction between Gallic Acid and Lysozyme by Molecular Dynamics Simulation and Optical Spectroscopy. International Journal of Molecular Sciences, 2015, 16, 14786-14807.	4.1	21
38	A novel biodegradable hyperbranched polyester prepared from cellulose and tyrosine via the synthesis route of glycopeptides. Polymer Chemistry, 2015, 6, 2822-2826.	3.9	2
39	The activity of the artemisinic aldehyde Δ11(13) reductase promoter is important for artemisinin yield in different chemotypes of Artemisia annua L Plant Molecular Biology, 2015, 88, 325-340.	3.9	45
40	Evaluating the Environmental Health Effect of Bamboo-Derived Volatile Organic Compounds through Analysis the Metabolic Indices of the Disorder Animal Model. Biomedical and Environmental Sciences, 2015, 28, 595-605.	0.2	4
41	Effects of overexpression of AaWRKY1 on artemisinin biosynthesis in transgenic Artemisia annua plants. Phytochemistry, 2014, 102, 89-96.	2.9	83
42	Synthesis, characterization and properties of celluloseâ€grafted glycine derivatives. Journal of Applied Polymer Science, 2014, 131, .	2.6	5
43	Binding between lead ions and the high-abundance serum proteins. Chemosphere, 2014, 112, 472-480.	8.2	9
44	Trichome-specific expression of the amorpha-4,11-diene 12-hydroxylase (cyp71av1) gene, encoding a key enzyme of artemisinin biosynthesis in Artemisia annua, as reported by a promoter-GUS fusion. Plant Molecular Biology, 2013, 81, 119-138.	3.9	72
45	Studies on the Expression of Sesquiterpene Synthases Using Promoter-β-Glucuronidase Fusions in Transgenic Artemisia annua L. PLoS ONE, 2013, 8, e80643.	2.5	19
46	Trichome isolation with and without fixation using laser microdissection and pressure catapulting followed by RNA amplification: Expression of genes of terpene metabolism in apical and sub-apical trichome cells of Artemisia annua L Plant Science, 2012, 183, 9-13.	3.6	72
47	Structure of six anhydrous molecular salts assembled from noncovalent associations between carboxylic acids and bis-N-imidazoles. Journal of Molecular Structure, 2012, 1022, 220-231.	3.6	10
48	Transient Expression of Hemagglutinin Antigen from Low Pathogenic Avian Influenza A (H7N7) in Nicotiana benthamiana. PLoS ONE, 2012, 7, e33010.	2.5	41
49	Functional expression and characterization of sesquiterpene synthases from Artemisia annua L. using transient expression system in Nicotiana benthamiana. Plant Cell Reports, 2012, 31, 1309-1319.	5.6	21
50	Sesquiterpene coumarins. Phytochemistry Reviews, 2012, 11, 77-96.	6.5	54
51	Analysis of the spectroscopic characteristics on the binding interaction between tosufloxacin and bovine lactoferrin. Journal of Luminescence, 2011, 131, 768-775.	3.1	23
52	Structural Characterization of a Cu(I) Coordination Polymer Constructed by Weak Intermolecular Cu–Clâ<⁻Cl–Ar Interaction. Journal of Inorganic and Organometallic Polymers and Materials, 2008, 18, 300-303.	3.7	48
53	Study on the binding interaction between carnitine optical isomer and bovine serum albumin. European Journal of Medicinal Chemistry, 2008, 43, 2140-2148.	5.5	88
54	Electrochemical Characteristics of Gatifloxacin and Its Interaction with DNA. Analytical Sciences, 2006, 22, 685-689.	1.6	5

#	Article	IF	CITATIONS
55	Study on the Interaction between Pefloxacin Mesylate and Human Serum Albumin. Chinese Journal of Chemistry, 2005, 23, 37-43.	4.9	8
56	Binding Interaction of Gatifloxacin with Bovine Serum Albumin. Analytical Sciences, 2004, 20, 465-470.	1.6	110
57	A Quantitative Structureâ^'Property Relationship Analysis of logP for Disubstituted Benzenes. Journal of Physical Chemistry A, 2002, 106, 11550-11557.	2.5	27